Observations on "Mg" incorporated oxides of tungsten for superconducting applications

K. C. Ramesh Babu[a], A. Panneerselvam[b*], S. Mageswari[c], V. Hariharan
[a]*Department of Physics, Vivekanandha College of Technology for Women, Elayampalayam, Tiruchengode, Namakkal-637205, Tamilnadu, India*
[b*]*Department of Physics, Vivekanandha College of Engineering for Women(Autonomous),Elayampalayam, Tiruchengode, Namakkal-637205, Tamilnadu, India*
[c]*Department of Chemistry, Vivekanandha College of Engineering for Women(Autonomous),Elayampalayam, Tiruchengode, Namakkal-637205, Tamilnadu, India*
[d]*Department of Physics, Mahendra Arts and Science College.Kalippatti, Tiruchengodu, Namakkal–637501, Tamil Nadu, India*

The present work involves in the synthesis and characterization of pristine and "Mg" associated $WO_3.H_2O$ nano powders by a high yield irradiation technique using microwaves. The diffraction patterns present phased orthorhombic phase and retained even after annealing process. Clear evidence noticed for pure and doped samples in morphological behavior of the samples. The change in optical properties in terms of energy values revealed the contribution of dopants with the evident at 360 nm wavelength blue shift. The obtained magnetic behavior on the annealed samples revealed the transition offer magnetic state to diamagnetic state may be investigated for super conducting applications.

(Received January 22, 2024; Accepted April 18, 2024)

Keywords: Metel oxides, Dopant, Superconductors, Nanomaterials, Irradiation

1. Introduction

Superconductivity, the phenomenon of zero electrical resistance, has revolutionized various fields such as energy transmission, magnetic levitation, and high-speed computing. Tungsten oxide (WO_3) nanoparticles have garnered significant attention as a promising material for superconducting applications due to their unique electronic and structural properties. In recent years, researchers have explored various synthesis methods to enhance the superconducting properties of WO_3 nanoparticles, including doping and novel fabrication techniques. By systematically investigating the microwave-assisted synthesis and doping of WO_3 nanoparticles, this study aims to contribute to the development of advanced superconducting materials for various applications. The observations and results from various research may focus on design and optimization of oxide based superconducting devices, Hence it will lead further by understanding practical and efficient current superconducting technologies. To support this, Nano particles are being focused in various specialized areas with its corresponding large surface area. As on date, nano particles with high surface energy are being involved in wide range of applications. Ex: catalysis, window technology, food industries, cosmetics and medicals [1]. In particular, an hydrated tungsten oxides are recently focused for the developments of windows [2], catalysis [3], luminescent [4] and chemical, bio and gas sensors [5]. Polymorphism and oxygen deficiencies support this kind of materials for various applications. Moreover, the corresponding physical and chemical properties of the samples with respect to the dimensionat nano level are being utilized for many applications.

*Corresponding author: kcrbphy@gmail.com
https://doi.org/10.15251/DJNB.2024.192.641

Moreover, various novel synthesis methods with the aid of dopants (metalic elements)are contributing to lead the host materials at nano level with higher surface energies to tune relatively better physical and chemical properties. Hence, Focus is being kept on synthesis methods as thin films, nano powders [6-11] etc. However, cost effective with high yields to be focused more, hence, new synthesis methods are introduced with sufficient arrangements to satisfy particular applications. Recently, Prepared pure and copper associated WO_3 nano materials to detect volatile organic gases. [12]. Pure and Zinc doped thin films ofWO_3 utilized for analyzing photocurrent and photo related activities [13].

In addition with the above, chromium doped porous anhydrated oxide of tungsten adopted to analyze amines based compounds for better sensitivity [14]. Analyzis on "Au" incorporated nano scale materials using simple colloidal chemical method to detect Nitrous oxide at low temperature [15]. Pristine and "Ti" added WO_3thin films resulted better conductivity in ambient atmosphere [16].

Hence, we aim to analyze the role of dopants and method on "Mg" incorporated anhydrous tungsten oxide nanoparticle as high efficient superconductors.

2. Experimental procedure

Pristine and "Mg" doped $WO_3.H_2O$ nano scale materials were synthesized by irraidating using microwaves at ambient condition [17]. In this present method, Analytical grade of around tungstic acid was dissolved sodium hydroxide (NaOH) for around 20ml solution. The yellow coloured solution was further stirred for 20 min in ambient conditions. This formation of the products may be due to exchange of protons according exchange protocol [18]. Followed by the above procedure, Magnesium chloride ($MgCl_2$; 2 & 5 wt.%) was allowed into tungstic acid (H_2WO_4) to make 20ml solution. The resultant solution was slowly mixed once again for further 20 minutes in air atmosphere. The pH of the solution was measures as 7.0 due to the mixed solution and it was changed to 1 by mixing concentrated Hydro Choleric acid (HCl) because it is the agent for precipitation and also will be a platform for fixing the morphology of the end products [19]. The final solution transferred into an oven (Microwave frequency: 2.45GHz with 900 W) and maintained at 10 min under 600 W. The final products were transferred to muffle furnace and maintained at 600ºC/6h/air to eliminate the impurites and improving the quality of the product in terms crystallinity.

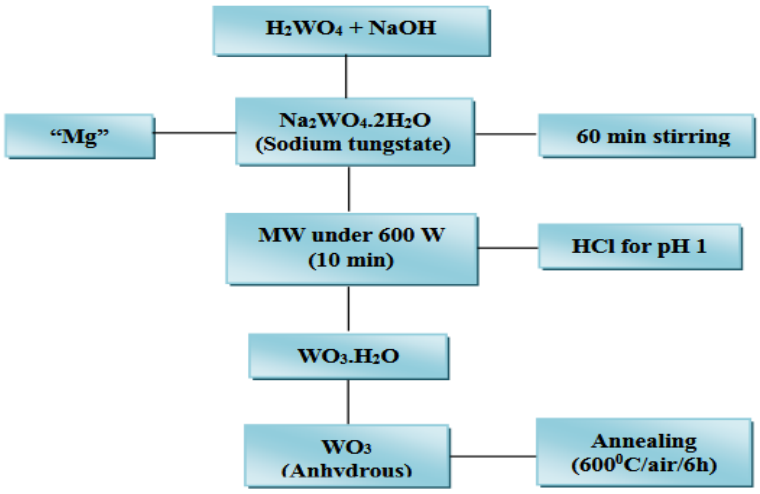

Fig. 1. llustration of the synthesis procedure.

2. Characterizations

2.1. X-ray diffraction analysis

Pristine and doped anhydrate tungsten oxide nanoparticles, XRD analysis can provide valuable information about their crystalline structure, lattice parameters, and phase purity. Let's discuss how XRD analysis can be employed to investigate pure and doped WO_3 nanoparticles. XRD analysis can quantitatively determine the phase composition of the pure and doped WO_3 nanoparticles. This analysis involves measuring the intensity of the diffraction peaks and comparing them with the standard intensity values for different phases. The quantitative phase analysis can reveal the relative abundance of each phase in the sample.

Fig.2 revealed the diffraction pattern for corresponding Pristine and metal incorporated as dopants in both pure and doped H_2O incorporated anhydrous tungsten based oxide with Fig. 3 dipicts the respective model for treated sample. The results confirmed the formation of hydrated tungsten oxide with high crystalline nature and also in agreement with JCPDS (43-0679 - Orthorhombic). A negligible amount of shift in diffraction in the case of doped sample revealed the presence of dopant as ions at the lattice site of $WO_3.H_2O$ due to size of the incorporated "Mg" ion. Moreover, for manganese (5Wt. %) produced a change in plane (020) proved the dopant in the crystalline units of WO^{2-}.

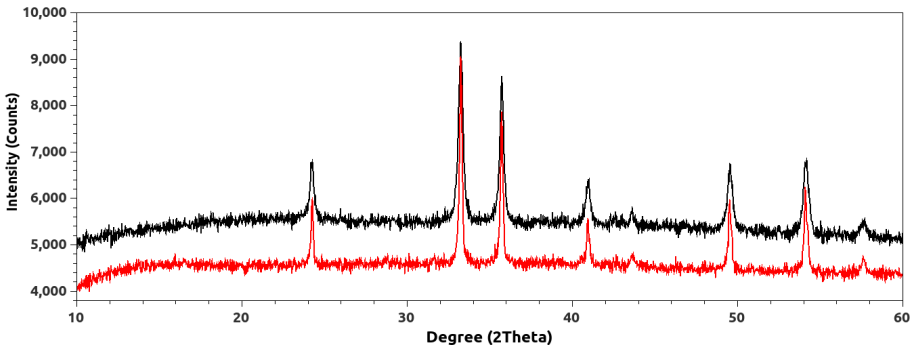

Fig. 2. XRD profiles of pure and doped $WO_3.H_2O$.

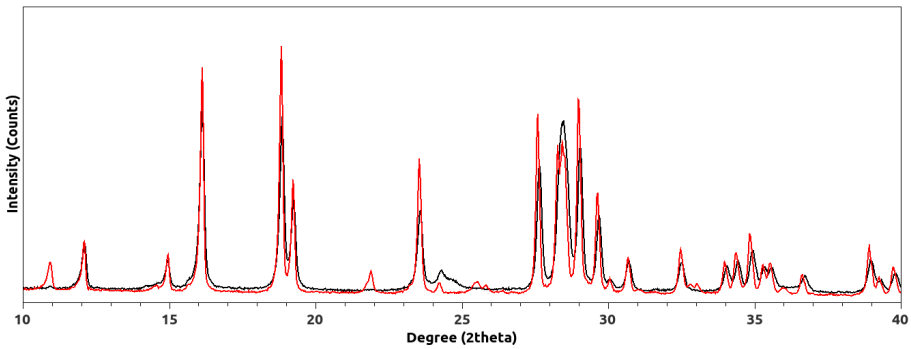

Fig. 3. XRD profiles of pure and doped WO_3.

3. Microscopic observation (FE-SEM)

Microscopic observation using Field-Emission Scanning Electron Microscopy (FE-SEM) is a powerful technique for analyzing the surface morphology, particle size, and distribution of pure and doped tungsten oxide (WO_3) nanoparticles. FE-SEM provides high-resolution imaging, allowing for a detailed examination of the nanoparticles at the micro- and nanoscale. Here's how FE-SEM can be utilized to observe pure and doped WO_3 nanoparticles. FE-SEM images can

provide insights into the agglomeration or dispersion behavior of WO_3 nanoparticles. The presence of agglomerated particles indicates poor dispersion, which can affect the overall properties and performance of the nanoparticles. Doping may influence the agglomeration behavior, and FE-SEM images can help assess the effectiveness of doping in improving dispersion. The microscope analysis on pure and doped tungsten oxides with reference to aluminum as substrate presented in Fig. 4. The photographs reflects the occurance of spheres with more non uniformity in morphology with 0.8 – 3 μm in long and 1 - 2 μm along minor axis. The close analysis on the surface having parallel plates like arrangements indicated that the units growth along b axis (020) in agreement with the diffraction analysis.

Fig. 5 shows the photographs of anhydrated tungsten oxides with the same as pristine with 4 – 5μm in lateral axis and 2-3μm in the longitudinal axis. This may be because of the agglomeration due to the re crystallization process and during this process fast collusion maybe occurred in crystallization in the desired atmosphere also because of the annealing effect. The occurrence of prominent crystalline nature when compare to that of without doped sample explored the incorporation of metals as dopant especially on the annealed samples.

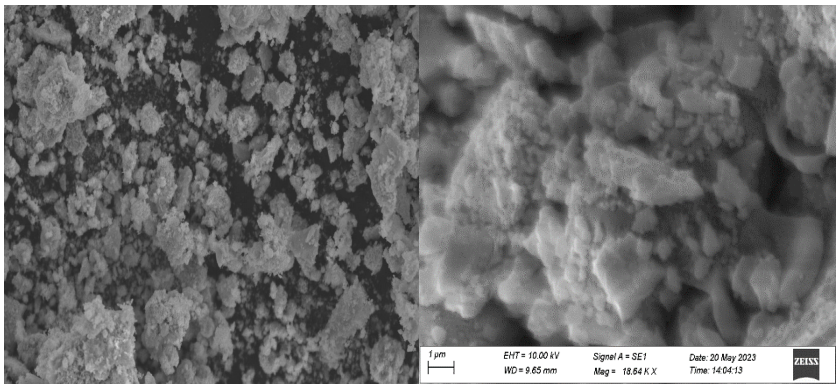

Fig. 4. Micrographs of hydrated tungsten oxide.

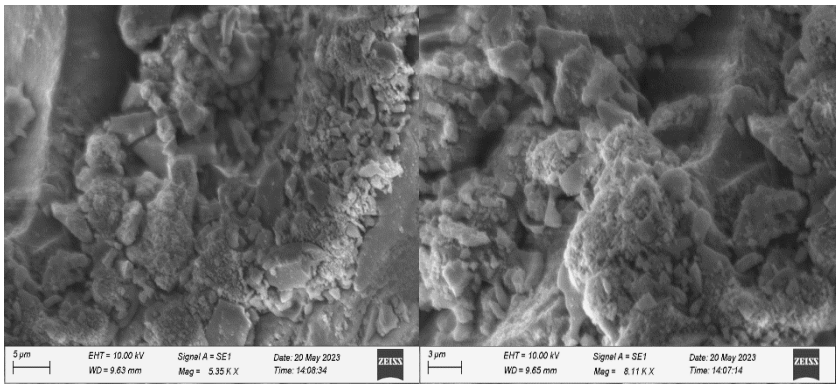

Fig. 5. Micrographs of a hydrated tugnsten oxide.

4. Optical properties

The corresponding optical properties of the pure and doped samples are shown in Fig. 6throughdiffusionreflectancespectroscopy.Thereflectancepeaksaroundtheregion 520-600nm with the maximum intensities occurred during reflection that moved towards blue in the case of as prepared sample and red for treated samples at 600^0C observed in the end products. The band gap energies were calculated using Kubelka-Munk (KM) model which is.

$$\frac{K}{S} = \frac{(1-R)^2}{2R_\infty} = F(R)$$

F® is noted as remission or KM function, where

$$R_\infty = \frac{R_{sample}}{R_{std.}}$$

To calculate the respective band gap energies of the end products, a graph is to be plotted such as $[F(R_\infty)h\gamma]^2$Vs $h\gamma$ and the corresponding intercept value at x axis will resulting the respective bandgap energy Eg of the individual sample [20]. The values for band gap energies were 3.27 and 3.33 eV respectively. This may be Burstein-Moss (BM) [21] effect. According to this effect the blocking of conduction band that allows only above Fermi level to unblocked valance level (between W^{6+} to Mg^{2+}) due to the incorporation of Mg^{2+}ion in intermediate energy levels[22].

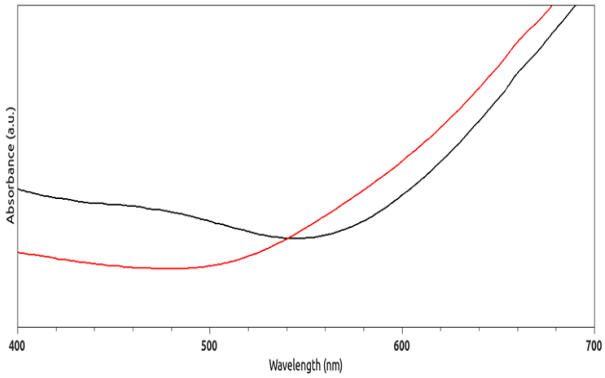

Fig. 6. Optical analysis of WO_3 (pure and doped).

4.1. Surface energy analysis

The theory associated in order to find the surface energies of the prepared products was BET analysis. It was observed that annealed sample $W_{17}O_{47}$ as discussed in elsewhere is having larger surface area (68.14 $m^2.g^{-1}$) when compared to that of remaining prepared samples. Also, it is interested to observe that the identified value is very much higher than that of commercially available WO_3 (36.56 $m^2.g^{-1}$) as reported. Pure $WO_3.H_2O$, $WO_3.H_2O$ (Mg~3wt.%) and WO_3(Mg~3wt.%) are having significant surface area such as 33.35$m^2.g^{-1}$,5.22$m^2.g^{-1}$and29.22$m^2.g^{-1}$ respectively. From these observations it is clear that the large surface area obtained in the case of pure annealed sample ($W_{17}O_{47}$) may be attributed to the introduction of abundance oxygen vacancies during the treatment of annealing of $WO_3.H_2O$ also may be due to ordering of phase transition from $WO_3.H_2O$ to $W_{17}O_{47}$. Also it demonstrates the contribution of oxygen vacancies that may fix the surface energies of the prepared samples.

4.2. Raman analysis

Raman spectroscopy can help determine the crystal structure and phase transitions in WO_3 nanoparticles. Different crystal structures of WO_3, such as monoclinic, orthorhombic, and hexagonal, exhibit distinct Raman signatures. By comparing the obtained Raman spectra with reference spectra of known crystal structures, the crystal structure of the nanoparticles can be identified. Additionally, Raman spectroscopy can detect phase transitions, such as the transition between the monoclinic and orthorhombic phases, by observing changes in peak positions, intensities, or the emergence of new peaks. Fig. 7 displays Raman spectra of Pristine and “Mn” doped WO_3. In general, peaks appeared from 200 to 350 cm^{-1} and 650 to 900 cm^{-1} belongs to O-

W-O bending modes and W-O stretching vibrations of WO_3 system. This is in good agreement with powder XRD observations. During the introduction of dopants into lattice, the peak intensity reflected a rise in counts is ascertained by Mn doping effect [23].These observations contribute to a comprehensive understanding of the structural and vibrational characteristics of the nanoparticles, aiding in the design and optimization of WO_3-based materials for various applications, including superconducting technologies.

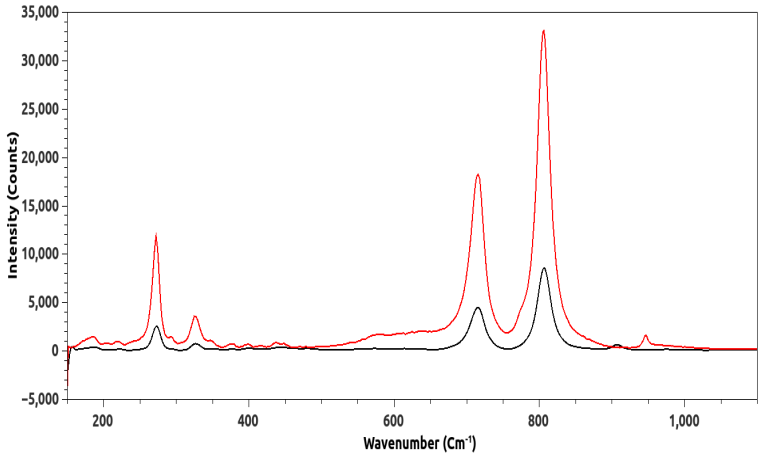

Fig. 7. Raman spectra on pure and doped WO_3.

4.3. Magnetic behavior (VSM) analysis

The magnetic behavior analyzed using VSM for undoped and Magnesium incorporated tungsten oxide (WO_3) at ambient condition reflected in Fig.8. This studies were carried out on the annealed samples at room temperature, Moreover, it is to be noted that the products were with oxygen deficient nature or else non stoichiometric tungsten oxide with diamagnetic behavior, making it suitable for superconducting applications [24], The unpaired electrons in holes rich regions for oxygen deficient samples that may enhanced the ferromagnetic behavior with the diamagnetic nature. These interesting findings propose that the "Mg" incorporated samples try to avoid diamagnetic states or other words superconducting state. Also, the dopant try to fix the oxygen deficient of end products especially in the case of samples maintained at appropriated annealed temperature.

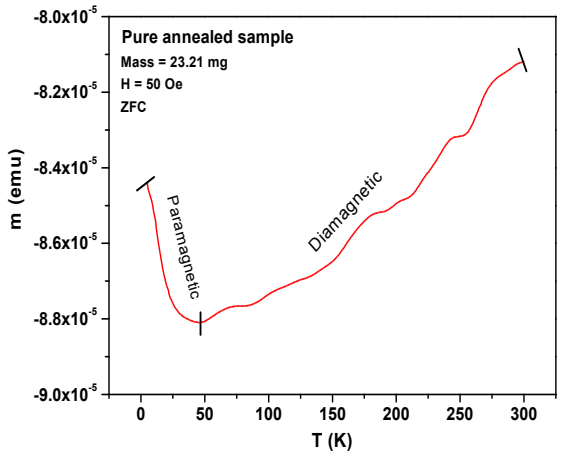

Fig. 8. Magnetic responses on pure and doped WO_3.

Conclusions

The authors having aim to introduce a novel material for superconducting applications using pure and "Mg" doped tungsten oxides by the irradiation technique with the aid of microwaves. Diffraction analysis confirmed the formation of orthorhombic phase. On the other hand, annealed samples also retained the same orthorhombic which were also confirmed through diffraction analysis. The interesting results obtained for "Mg" incorporated samples due to its oxygen deficient nature. Optical analysis in the regions of UV – VIS and NIR will be the evidence in terms of optical properties especially on the heat treated samples to confirm presence of foreign atoms in tungsten oxide crystals. From these observation, interesting results from VSM suggested that the samples prepared for superconducting applications with diamagnetic state (Mg doped sample) noteworthy material for superconducting applications due to its oxygen deficiencies (alternate the mole fraction of the oxygen).

References

[1] Charles P. Poole, Frank J. Owens. Nature (2003) 1-20.
[2] Ygao, Ybando. Nature (2003) 71-110.
[3] Nanosystem; Molecular Machinery, manufacturing and computation, (2006) 0-471.
[4] Hari Singh Nalwa, Nanostructured materials and nanotechnology, Academic Press, London, (2002).
[5] S. K. Singh, S. Basu, Materials chemistry and physics. 20 (1998) 381-396; https://doi.org/10.1016/0254-0584(88)90076-4
[6] Dubois, Hans F.W., Quality Management in Health Care, 10(2) (2002) 47-57; https://doi.org/10.1097/00019514-200210020-00009
[7] Rachel Heil Wentworth Institute of Technology (2007) Dept of Electronics and Mechanical.
[8] Boris Lamontagne et al., The next generation of switchable glass: the Micro-Blinds, (2009) 637-639.
[9] Tungsten trioxide Properties, The Merck Index, Vol 14, 2006.
[10] Rosen MJ (2004), Surfactants and Interfacial Phenomena (3rd ed.). Hoboken, New Jersey: John Wiley & Sons; https://doi.org/10.1002/0471670561
[11] J. Wang, C. Wu, Ning Hu, Jie Zhou, Liping Du, Ping Wang, Biosensors 2(2) (2012) 127-170; https://doi.org/10.3390/bios2020127
[12] K. Jameson, D. Rogers Christopher, D. Guzman Noah, Taylor Srivatsan Raman Kelley, Anderson George, M. Church, Nucleic acid research 15(43) (2015) 7648-7660; https://doi.org/10.1093/nar/gkv616
[13] Parikha Mehrotra, Journal of Biology and Craniofacial Research 6 (2016) 153-159; https://doi.org/10.1016/j.jobcr.2015.12.002
[14] I. Celine, L. Justino, C. Armando, Duarte, A. P. Teresa, Rocha-Santos, Sensors, 17(12), (2017); https://doi.org/10.3390/s17122918
[15] M. Pilo, R. Farre, J. Izabela, Lchowicz, E. Masolo, A. Panzanelli, G. Sanna, N. Senes, A. Sobral, N. Spano, J. Anly. Methd. in Chemistry (2018); https://doi.org/10.1155/2018/1849439
[16] Csaba Balazsi et al., Journal of the European Ceramic Society.28 (2008) 913-917; https://doi.org/10.1016/j.jeurceramsoc.2007.09.001
[17] Lídia Santosa, Celia Silveira, Elamurugu Elangovan, Joana P. Netoa, Daniela Nunesa, Luis Pereiraa, Rodrigo Martinsa, Jaime Viegasd, Jose J.G. Mourab, Smilja Todorovicc, M. Gabriela Almeidab,e, Elvira Fortunatoa, Sensor and Actuators B, (2015); https://doi.org/10.1016/j.snb.2015.09.046
[18] L. Santos, C. M. Silveira, E. Elangovan, J.P. Neto, D. Nunes, L. Pereira, R. Martins, J. Viegas, J. J. G. Moura, S. Todorovic, M. G. Almeida, E. Fortunato, CENIMAT, 223 (2016) 186-194; https://doi.org/10.1016/j.snb.2015.09.046

[19] C. Anitha, K. Asokan, C. Sekar, Sensor and Actuators B, 238 (2017) 667 – 675; https://doi.org/10.1016/j.snb.2016.07.098
[20] Govindhan Maduraiveeran, Manickam Sasidharan, Vellaichamy Ganesan, Biosensor and Bioelectronics, 103 (2018) 113-129; https://doi.org/10.1016/j.bios.2017.12.031
[21] Baig.U, Gondal M.A., SuriyaRehman, Sultan Akhtar, Appl. Nanosci. 2020,10,851-860; https://doi.org/10.1007/s13204-019-01186-z
[22] L. R. Dai, J. Zhou, X. F. Gao, J. B. Li, B. Y. Feng, Y. Z. Yao, Y. M. Wang, W. W. Cui, X. J. Li, Digest Journal of Nanomaterials and Biostructures, 2022, 17, 1125-1134. https://doi.org/10.15251/DJNB.2022.174.1125.
[23] Duan. G, Chen. L, Jing. Z,Luna. P. D., Wen. L, Zhang. L,Zhao. L, Xu. J, Li. Z, Yang. Z, Zhou. R, Chem. Res. Toxicol. 2019, 32(7), 1357-1366; https://doi.org/10.1021/acs.chemrestox.8b00399
[24] Matharu.R.K., Ciric.L, Ren.G, Edirisinghe.M, Nanomaterials 2020,10,1017,1-16; https://doi.org/10.3390/nano10061017